Carbon-Nanotube-Embedded Hydrogel Sheets for Engineering Cardiac Constructs and Bioactuators

Su Ryon Shin,[†,×,‡] Sung Mi Jung,[§] Momen Zalabany,[†,‡] Keekyoung Kim,[†,‡] Pinar Zorlutuna,[†,‡] Sang bok Kim,[†,‡] Mehdi Nikkhah,[†,‡] Masoud Khabiry,[⊥,∥] Mohamed Azize,[§] Jing Kong,[§] Kai-tak Wan,[⊥] Tomas Palacios,[§] Mehmet R. Dokmeci,[†,×,‡] Hojae Bae,[¶] Xiaowu (Shirley) Tang,[△,*] and Ali Khademhosseini[†,×,‡,*]

[†]Center for Biomedical Engineering, Department of Medicine, Brigham and Women's Hospital, Harvard Medical School, 65 Landsdowne Street, Cambridge, Massachusetts 02139, United States, [×]Wyss Institute for Biologically Inspired Engineering, Harvard University, Boston, Massachusetts 02115, United States, [‡]Harvard—MIT Division of Health Sciences and Technology and [§]Department of Electrical Engineering and Computer Science, Massachusetts Institute of Technology, Cambridge, Massachusetts 02139, United States, [⊥]Bioengineering Program and [∥]Mechanical and Industrial Engineering, Northeastern University, Boston, Massachusetts 02115, United States, [¶]Department of Maxillofacial Biomedical Engineering and Institute of Oral Biology, School of Dentistry, Kyung Hee University, Seoul 130-701, Republic of Korea, and [△]Department of Chemistry, University of Waterloo, Waterloo, Ontario N2L 3G1, Canada

ABSTRACT We engineered functional cardiac patches by seeding neonatal rat cardiomyocytes onto carbon nanotube (CNT)-incorporated photo-cross-linkable gelatin methacrylate (GelMA) hydrogels. The resulting cardiac constructs showed excellent mechanical integrity and advanced electrophysiological functions. Specifically, myocardial tissues cultured on 50 μm thick CNT-GelMA showed 3 times higher spontaneous synchronous beating rates and 85% lower excitation threshold, compared to those cultured on pristine GelMA hydrogels. Our results indicate that the electrically conductive and nanofibrous networks formed by CNTs within a porous gelatin framework are the key characteristics of CNT-GelMA leading to improved cardiac cell adhesion, organization, and cell—cell coupling. Centimeter-scale patches were released from glass substrates to form 3D biohybrid actuators, which showed controllable linear cyclic contraction/extension, pumping, and swimming actuations. In addition, we demonstrate for the first time that cardiac tissues cultured on CNT-GelMA resist damage by a model cardiac inhibitor as well as a cytotoxic compound. Therefore, incorporation of CNTs into gelatin, and potentially other biomaterials, could be useful in creating multifunctional cardiac scaffolds for both therapeutic purposes and *in vitro* studies. These hybrid materials could also be used for neuron and other muscle cells to create tissue constructs with improved organization, electroactivity, and mechanical integrity.

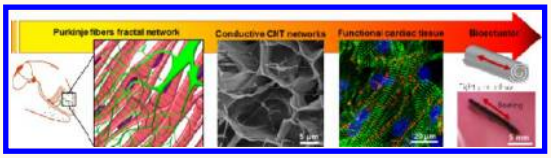

KEYWORDS: carbon nanotubes · gelatin · hydrogel · cardiac tissue engineering · bioactuator

Development of biomimetic extracellular matrices (ECMs) is of great importance in myocardial tissue engineering.[1] Macroporous scaffolds, made of either biocompatible natural or synthetic polymers such as alginate,[2] gelatin,[3] and poly(glycerol sebacate) (PGS),[4] have been the most commonly used ECMs. Significant progress has been made in engineering cardiac tissues on such scaffolds, with the hope to eventually develop functional substitutes to replace damaged heart tissues. However, major challenges remain, and further improvement in biomimetic scaffold design remains an area of intensive research. Compared to the native heart tissue microenvironments, the macroporous scaffolds possess a few key characteristics that are "unnatural". First, the scaffolds are electrically insulating at biologically relevant frequencies (DC to a few hertz), while heart muscles have a DC conductivity around 0.1 S/m and are underlined with electrically conductive purkinje fibers.[5,6] Second, many scaffolds lack nanofibrous architectures at submicrometer scale (10—100 nm in diameter), which are abundant in native ECMs and play a key role in regulating cellular behavior. Third, the scaffolds are typically mechanically weaker than the native heart tissues. Recently, a few studies have been reported to address the unnatural traits of polymer macroporous scaffolds by incorporation of nanomaterials. For example, polymers impregnated with gold nanostructures were shown to improve electrical signal propagation and enhance cellular excitability of both cardiomyocytes and neurons.[5,7] In addition, hybrid materials incorporating nanofibers were shown to

* Address correspondence to alik@rics.bwh.harvard.edu, tangxw@uwaterloo.ca.

Received for review December 1, 2012 and accepted January 28, 2013.

Published online January 30, 2013
10.1021/nn305559j

improve cell adhesion, viability, and direct cells to self-assemble in three dimensions.[8,9] Each of these recent studies led to meaningful strategies to tackle one of the three traits listed above, but not all. For instance, Au nanowires improved electrical conductivity of alginate scaffolds, but no enhancement to the scaffold elastic compressive modulus was observed.[7] Further, nanoparticles tend to aggregate into isolated microstructures, which might introduce stress centers leading to fracture after strong contractile beating.

Here, we report a hybrid scaffold, with carbon nanotubes (CNTs) homogeneously incorporated into a gelatin derivative, which could simultaneously address the aforementioned three drawbacks of polymer porous scaffolds while maintaining their beneficial properties, such as high porosity, biocompatibility, and biodegradability. Due to the fibrous morphology, high electrical conductivity, and high mechanical strength of CNTs,[11] we hypothesize that CNTs can lead to extensive nanofibrous networks embedded in the porous gelatin framework, which not only strengthen the scaffold mechanically but also reduce the electrical impedance.[12,13] In a recent study, a CNT-based polylactic acid scaffold was shown to induce cardiac differentiation of mesenchymal stem cells (MSCs), which indicated the possibility to promote electroactive tissue repair using CNTs.[14] The fractal-like CNT networks could also alter tissue organization and phenotype. Furthermore, the mechanically enforced scaffold could allow the fabrication and handling of ultrathin cardiac tissue patches, which are particularly suitable as cell delivery systems for cell therapy[15] and as soft actuators for *in vitro* biorobotic applications.[10,16]

Gelatin, which is the denaturized collagen, contains abundant cell binding sequences and has bioactivity similar to that of collagen.[17] By addition of methacrylate (MA) to the amine-containing side groups of gelatin, a photo-cross-linkable derivative (GelMA) can be made.[18] Previous work by our team demonstrated GelMA as an attractive scaffold material for creating micropatternable 3D tissue constructs.[19,20] We also reported recently the incorporation of CNTs up to 0.5 mg/mL into 5% GelMA (*i.e.*, CNT-GelMA) and showed that CNTs enhanced the mechanical properties of GelMA hydrogels while preserving their porosity and biodegradability, evaluated using 3T3 fibroblasts and hMSCs.[21] Surface-functionalized CNTs showed no cytotoxicity[22,23] and have been explored for drug delivery,[24] imaging,[25] and cancer therapy[26] by various research groups. In previous studies, solid substrates coated with pristine CNTs[27−29] or CNT/PLGA nanofibers[9] were shown to promote electrical signaling among cultured cardiomyocytes and neurons. Overall, existing literature reports consistently indicate that the incorporation of CNTs into GelMA can be a promising approach to design high-performance cardiac scaffold materials. In this work, we explored CNT-GelMA hybrid gel films as pseudo-3D scaffolds with high concentrations of CNTs (up to 5 mg/mL). The correlation between CNT concentration and physiological characteristics of cultured cardiac tissues was systematically evaluated. Plus, we investigated the multifunctional nature of the CNT-GelMA scaffolds, which provide structural support to seeded cardiac cells, improve tissue morphogenesis, and act as scavengers of free radicals[30−32] to protect cultured cardiac tissues.

RESULTS AND DISCUSSION

Fabrication and Physical Properties of the CNT-GelMA Hydrogel. Thin films of CNT-GelMA hybrid hydrogel with a typical thickness of 50 μm were prepared by UV irradiation of CNT-containing prepolymer solutions sandwiched between two glass slides. Details are presented in the Experimental Methods section and schematically illustrated in Figure 1B and Supporting Information Figure S1. GelMA-coated CNT fibers with diameters in the range of 50−100 nm were shown to be homogeneously dispersed in the prepolymer solution (Figure 1C). SEM images of gelatin film surfaces showed that CNT-GelMA had porosity and pore size distribution similar to that of the pristine GelMA, but with fibrous meshworks interconnecting pores (Figure 1D,E), which appeared similar to the purkinje fiber networks on the surface of heart muscle fibers (Figure 1A). The formation of the CNT meshworks can be attributed to the cross-linking of GelMA-coated CNTs (Figure 1D) *via* the acrylic groups. Higher CNT concentrations were observed to lead to higher densities of CNT fibers (Figure S2).

We evaluated the physical properties, specifically, compression modulus and electrical conductivity of the CNT-GelMA hybrids. The compressive modulus of the hydrogel is a key indicator of its ability to accommodate compressive strain from cardiac beating. The incorporation of homogeneously distributed CNT meshworks in macroporous hydrogel led to an increase in compression modulus from 10 kPa to a maximum of 32 kPa (Figure 1F). The Young's modulus of the CNT-GelMA gels, derived from the force-indentation data using a Hertzain model, is similar to that of the adult rat right ventricular myocardium (20 $\pm$ 4 to 54 $\pm$ 8 kPa)[4] and about 10 times higher than several other recently reported nanocomposite hydrogel systems, such as Au nanowire-incorporated alginate (3.5 kPa).[7] The continuous and branched CNT meshworks likely acted as reinforcements and therefore improved the mechanical stability of the hydrogel thin films. However, the trend in the increase of Young's modulus was only observed up to a concentration of 3 mg/mL. Further increase in CNT concentration led to mechanically weaker gels. This phenomenon can be explained by the high UV light absorption of CNTs (Figure S1), which caused a cross-linking gradient along the depth. Current exposure condition was optimized to maximize cross-linking at the upper portion of

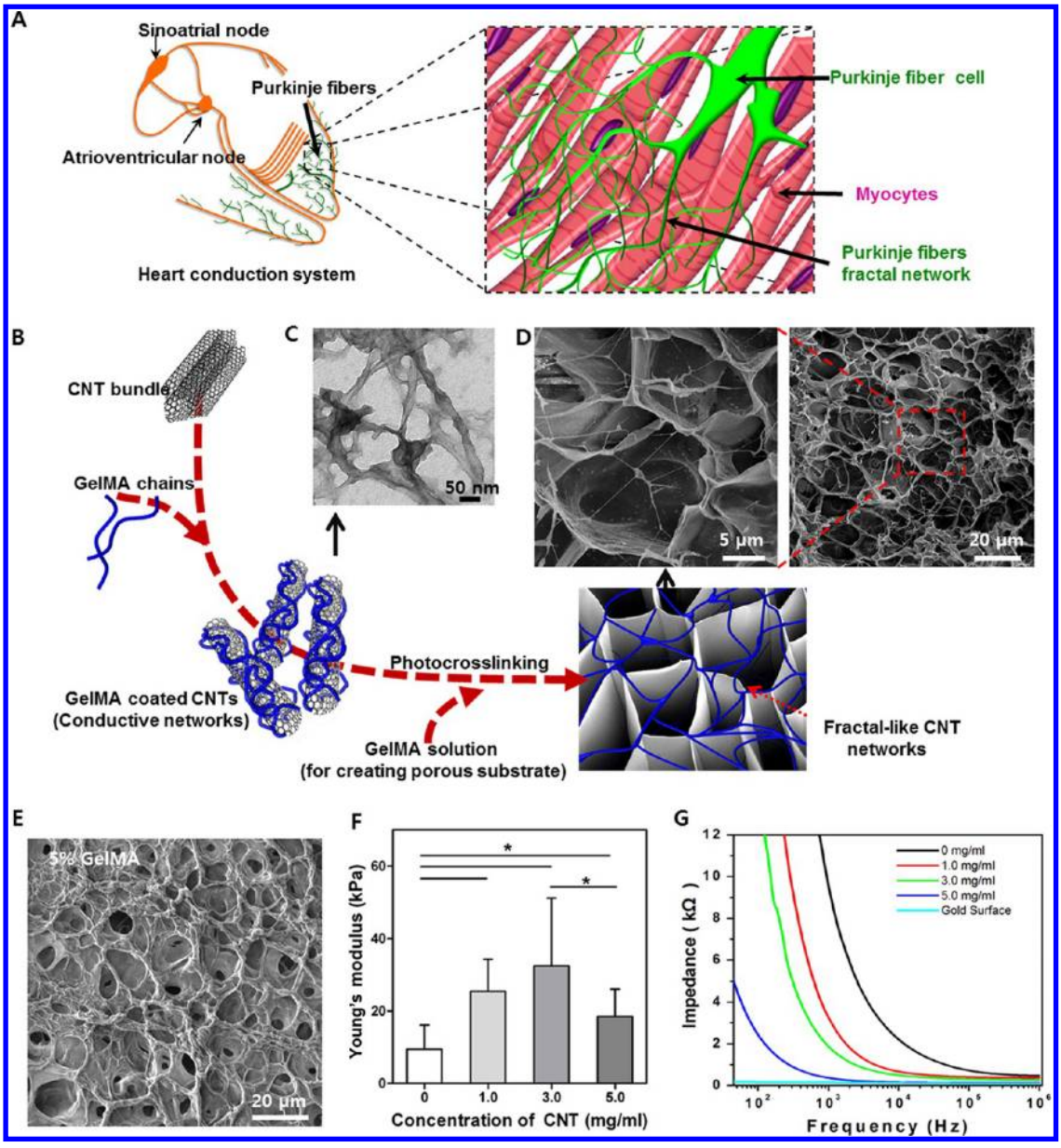

Figure 1. Structural, physical, and electrical characteristics of CNT-GelMA hydrogels. (A) Schematic diagram illustrating the isolated heart conduction systems showing the purkinje fibers, which are located in the inner ventricular walls of the heart. Heart muscle with purkinje fiber networks on the surface of the heart muscle fibers. (B) Preparation procedure of fractal-like CNT networks embedded in GelMA hydrogel. (C) TEM image of GelMA-coated CNTs. (D) SEM images show porous surfaces of a 1 mg/mL CNT-GelMA thin film. Magnified image shows nanofibrous networks across and inside a porous structure. (E) SEM images of pristine 5% GelMA. (F) Young's modulus of CNT-GelMA at fully swollen state varies significantly with CNT concentration (*$p < 0.05$). (G) Overall impedance of a 50 μm thick hydrogel thin film decreased drastically with increased CNT concentrations.

the 5 mg/mL thin films, which left the lower portion inefficiently cross-linked and rendered softer gels overall.[21]

All hydrogels, with and without CNTs, exhibited low impedance at high frequencies (above 0.1 kHz) due to capacitive currents. At lower frequencies, which are more physiologically relevant, the impedance of CNT-GelMA was significantly lower than that of pristine GelMA hydrogels (Figure 1G), a finding attributable to resistive currents through the bridging nanotubes. Previous reports have shown evidence that conductive scaffolds are superior to their more insulating polymer counterparts for improved electrical signal propagation among cardiac cells.[5,7] Therefore, we anticipate that CNT-GelMA hybrid gels, which are not only more electrically conductive but also stronger mechanically than GelMA hydrogels, can be a promising new scaffold material for engineering myocardial tissues.

Cardiomyocyte Viability and Organization on CNT-GelMA Thin Films. To assess the suitability of CNT-GelMA for the fabrication of cardiac patches, neonatal rat cardiomyocytes were seeded on CNT-GelMA thin films. Cell adhesion, viability, proliferation, and organization were

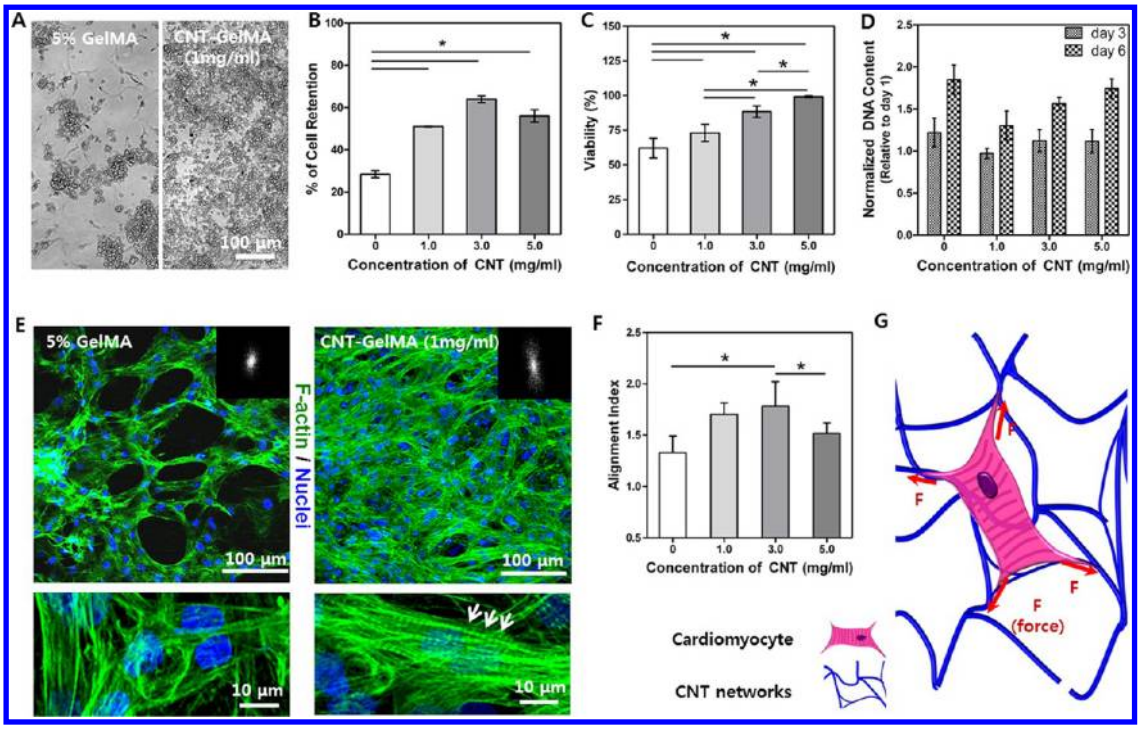

Figure 2. Improved cardiac cell adhesion, maturation, and alignment on CNT-GelMA. (A) Optical images of cardiomyocytes (day 1) revealed better cell retention and more homogeneous seeding on CNT-GelMA than on pristine GelMA. (B) Percentage cell retention and (C) viability one day after cell seeding on hydrogel surfaces showed strong dependence on CNT concentration (*$p < 0.05$). (D) Normalized DNA quantities on day 3 and day 6 were not obviously affected by CNT concentration. (E) Confocal images of cardiomyocytes after culturing for 5 days on pristine GelMA and 1 mg/mL CNT-GelMA revealed more uniform cell distribution and partial cell alignment on CNT-GelMA. F-actin and cell nuclei were labeled fluorescent green and blue, respectively. Insets are corresponding FFT images. Higher magnification images showed well-elongated cardiac cells and well-developed F-actin cross-striations (bottom right, white arrows) on CNT-GelMA but not on pristine GelMA (bottom left). (F) Alignment index derived from FFT images showed strong dependence on CNT concentrations (*$p < 0.05$). (G) Stretching force resulting from strong cell−CNT interactions could affect cardiomyocyte organization and promote myotube striation.

evaluated and compared to those on pristine GelMA hydrogel films. Still images taken one day after cell seeding and washing with culture medium showed homogeneous and interconnected cells covering the entire area of the CNT-GelMA surface but aggregated patches of cells on the pristine GelMA surface (Figure 2A). The percentage cell retention and viability (day 1) on CNT-GelMA were significantly higher than those on pristine GelMA (Figure 2B,C). Overall, these results suggest that CNT-GelMA is superior to pristine GelMA in terms of cell adhesion, spreading, retention, and viability. This is an important improvement since non-transformed cells are known to have high rate of apoptosis on soft substrates.[33] Furthermore, cellular DNA contents were measured to evaluate cell proliferation after day 1 (Figure 2D). Normalized DNA concentrations on day 3 and day 6 showed no significant dependence on CNT concentration. Therefore, CNTs promoted cell spreading and elongation but did not alter the proliferation of impurity cells, such as the small percentage of cardiac fibroblasts typically contained in the extracted cell population. In addition, no CNT cytotoxic effects were observed during the 7 day culture period.

Organization of cardiomyocytes on the CNT-GelMA surface was investigated after 5 days of culture under static conditions. Confocal fluorescence images of filamentous (F-) actin (green) and DNA (blue) labeled cardiac cells were observed forming tissue-like 2D constructs on both CNT-GelMA and pristine GelMA thin films (Figure 2E). Cardiac cells on pristine GelMA substrates were preferentially oriented in the plane of the thin film, but their arrangement within the plane is random and with certain aggregation. In comparison, cardiac cells on CNT-GelMA were clearly more homogeneous, intact, and locally aligned. At high magnification, well-elongated cardiac cells and cross-striations (Figure 2E, bottom right, white arrows) were observed on the CNT-GelMA surface which were absent on the pristine GelMA surface (Figure 2E, bottom left). Local cell alignment was further quantified by fast Fourier transform (FFT)-based image analysis of F-actin filament orientation. More details on the FFT analysis are available in Figure S4. The calculated alignment indexes for various CNT concentrations are shown in Figure 2F. The best alignment was obtained with 3 mg/mL CNT, which is about 1.75 times that on pristine GelMA. This result is consistent with our previous observations of 3T3 fibroblasts encapsulated in CNT-GelMA, which also showed partial alignment.[21] The alignment index *versus* CNT concentrations

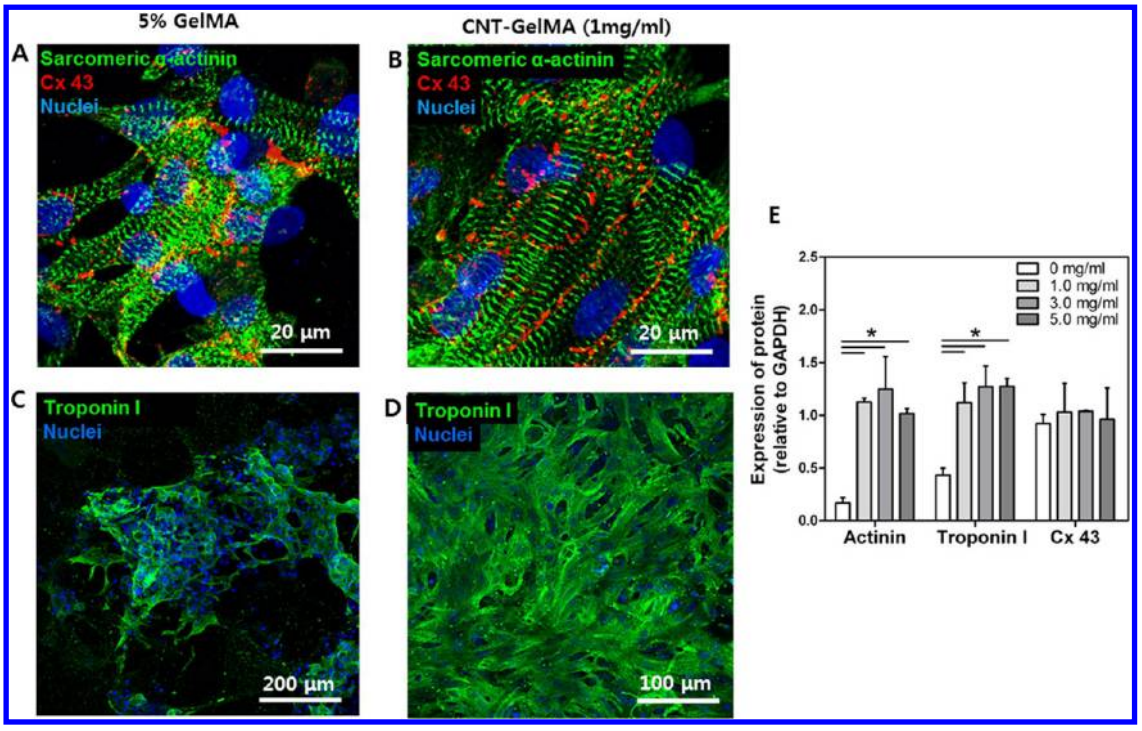

Figure 3. Phenotype of cardiac cells on CNT-GelMA hydrogels. Immunostaining of sarcomeric α-actinin (green), nuclei (blue), and Cx-43 (red) revealed that cardiac tissues (8 day culture) on (A) pristine GelMA and (B) CNT-GelMA were phenotypically different. Partial uniaxial sarcomere alignment and interconnected sarcomeric structure with robust intercellular junctions were observed on CNT-GelMA. Immunostaining of Troponin I (green) and nuclei (blue) showed much less and more aggregated Troponin I presence on (C) pristine GelMA than on (D) CNT-GelMA. (E) Quantification of α-actinin, Cx-43, Troponin I expression by Western blot (*$p < 0.05$).

followed the same trend as cell retention and compression modulus (Figure 2B,F and Figure 1F), suggesting that cell binding, cell density, and mechanical cue could all play an important role in regulating local cell organization in this case. Noteworthy is that surfaces with higher stiffness than 5% GelMA can be made without CNT and simply with increased GelMA concentrations (10 and 15%), while maintaining the same degree of methacrylation.[18] However, we observed no enhancement of spreading or organization of cardiomyocytes and HUVEC[18] on the surfaces made of 10 and 15% GelMA. This partially aligned behavior of cardiomyocytes might be related to the randomly distributed CNT meshworks in CNT-GelMA, which consisted of nanofibers with micrometer lengths and diameters in the range of 50−100 nm. These features resemble the physical traits of collagen fibrils in the native ECMs. Both randomly oriented and aligned nanofibers have been reported to guide cell interaction and organization and promote myotube striation (Figure 2G).[34] In addition, nanostructure impregnated composite/hybrid materials were shown to regulate essential cellular functions such as morphogenesis.[2]

Phenotype of the Engineered 2D Cardiac Tissue. On day 8, the phenotype of the *in vitro* cultured 2D cardiac tissues was evaluated by immunostaining of cardiac markers, sarcomeric α-actinin, Troponin I, and connexin 43 (Cx-43). Troponin I is involved in muscle calcium binding and contraction, while Cx-43 is responsible for cell−cell electrical and metabolic coupling. Compared to the cardiac tissues cultured on pristine GelMA, the 2D tissues on CNT-GelMA were shown to possess better defined, elongated, and more interconnected sarcomeric structures with partial uniaxial alignment (Figure 3A,B). Pervasive Troponin I expressions were also observed to be significantly higher by the tissues fabricated on CNT-GelMA (Figure 3C,D). Quantification of α-actinin, Cx-43, and Troponin I expressions was done by Western blot (Figure 3E), which revealed that the cardiac tissues cultured on CNT-GelMA had significantly higher levels of α-actinin (about 3.5 times) and Troponin I (about 1.5 times) relative to the tissues grown on pristine GelMA. The increase in Cx-43 expression, however, was only moderate. This is different from the much elevated Cx-43 levels observed on cardiac tissues cultured under electrical stimulation and on other conductive scaffolds.[5,7] Comparing the confocal images in Figure 3A,B, we conclude that, instead of an overall higher quantity of Cx-43, the much more homogeneously distributed Cx-43 and significantly higher number of cell junctions could benefit cell−cell coupling and enhance overall contractile properties of the cardiac tissues on CNT-GelMA. This hypothesis was supported by the strong synchronous beating observed.

Electrophysiological Properties of the Engineered 2D Cardiac Tissue. All tissues, on either CNT-GelMA or pristine

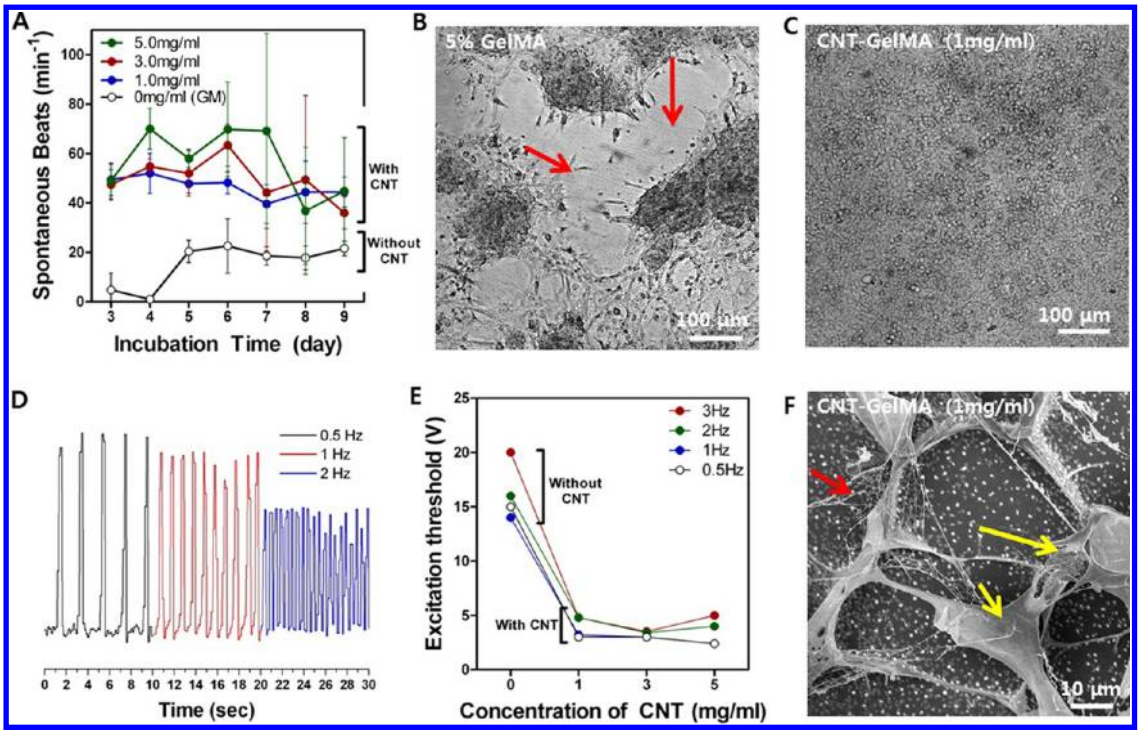

Figure 4. Improved mechanical integrity and advanced electrophysiological functions of cardiac tissues on CNT-GelMA. (A) Spontaneous beating rates of cardiac tissues recorded from day 3 to day 9 on a daily basis. Phase contrast images showed cardiac tissues ruptured on (B) pristine GelMA but intact on (C) CNT-GelMA on day 5. (D) Recording of synchronous beating signal of a tissue sample cultured on 1 mg/mL CNT-GelMA in response to applied external electric field at 0.5, 1, and 2 Hz. (E) Excitation threshold of cardiac tissues on CNT-GelMA was 85% lower than that on pristine GelMA. (F) SEM image shows morphology of cardiac cells cultured on CNT-GelMA. Red arrow: cytoplasmic prolongations adhered to CNT fibers. Yellow arrows: flat cell bodies.

GelMA, demonstrated spontaneous synchronous beating activity and were capable of being paced by electric field stimulation after as few as one day of culture. Spontaneous beating rates were recorded from day 3 to day 9 on a daily basis, as plotted in Figure 4A. Cardiac tissues cultured on CNT-GelMA showed a more stable spontaneous beating behavior, and the beating rate was on average (*e.g.*, 69.8 ± 19.1 BPM on day 6) 3 times those measured from tissues cultured on pristine GelMA (22.6 ± 11.1 BPM). CNT-GelMA exhibited much better mechanical integrity withstanding tissue contraction, as shown in the optical images taken on day 5. While severed pieces of tissues were observed on pristine GelMA (Figure 4B), tissues on CNT-GelMA remained intact (Figure 4C). Electric field stimulated contraction of the cultured cardiac tissues (up to 3 Hz) were also recorded (Figure 4D). Excitation thresholds were drastically reduced by the incorporation of CNTs, which were about 85% lower (Figure 4E). High electric potential is known to induce local pH gradient and gas generation on the surface of electrodes in an aqueous electrolyte, which causes damage to engineered cardiac tissues. The fact that we could control the beating behavior of cardiac tissues on CNT-GelMA with a considerably lower potential is advantageous in terms of avoiding such damage.

The overall enhanced electrophysiological functions of the CNT-GelMA-based 2D cardiac patches could result from a combination of several properties. One is the improved physical integrity of the CNT-GelMA thin films and thus the cardiac patches. Incorporation of CNTs strengthened the hydrogel mechanically (from 10 to 32 kPa) and improved cell adhesion. It has been suggested that increased stiffness in this range does not directly affect the beating behavior.[35] Rather, it affected cell phenotype[36] and rendered cardiac patches with better handling ability and less prone to rupture. The second is the better electrical cell−cell coupling enabled by more homogenously distributed cell−cell junctions and the conductive CNT meshworks. CNTs, bridging the insulating pore walls of the hydrogel, provided additional pathways for direct electrical current flow and reduced the impedance between cells for charge redistribution and action potential propagation. Similar mechanism accounted for the boost of neuronal signaling in a previous study.[28] The third is that the presence of nanofibrous CNTs promoted cardiomyocyte network, maturation, and alignment locally, as indicated by the partial alignment and cross-striation of F-actin, as well as the elevated expression of sarcomeric α-actinin and Troponin I. SEM analysis performed at high magnification revealed that the morphologies of the cardiomyocytes cultured on CNT-GelMA and pristine GelMA were distinctively different (Figure 4F). Physical contacts

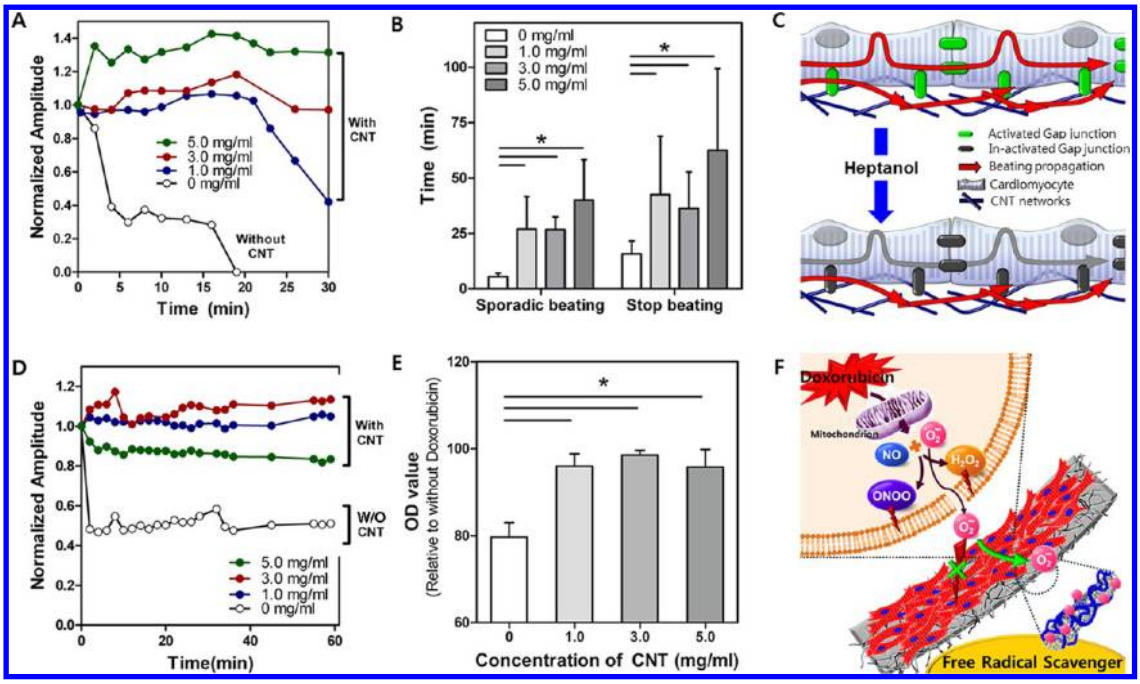

Figure 5. CNTs protected cardiac tissues against damages by heptanol and doxorubicin. Plots of spontaneous synchronous beating amplitude of cardiac tissues (5 day culture) on hydrogels with 0, 1, 3, and 5 mg/mL CNTs over time in response to (A) 4 mM heptanol and (D) 300 μM doxorubicin. (B) Time lapse before sporadic beating and stop beating induced by heptanol (*$p < 0.05$). (C) Schematic illustration of alternative electric signal propagation through CNT networks after inhibition of direct intercellular gap junctions by heptanol. (E) MTS data quantifying cell viability after 6 h exposure to doxorubicin (*$p < 0.05$). (F) Proposed mechanisms for CNTs to protect cardiac cells from damages caused by free oxygen radicals.

between the cell membranes and CNT nanofibers were clearly observed. On CNT-GelMA, cardiac cells were shown to have round cell bodies, measured to be approximately 10−15 μm in diameter, with nanoscale cytoplasmic prolongations adhered to CNT fibers. Both cell bodies and prolongations could be found intruding the base CNT-GelMA films, which therefore served as pseudo-3D scaffolds instead of 2D substrates. In contrast, cells on pristine GelMA had round cell bodies and no prolongations (Figure S7).

CNT-GelMA as a Protective Tissue Scaffold Material. We explored the potential of CNT-GelMA serving as protective cardiac scaffolds, which not only provided structural support but also prevented or reduced damage to cardiac tissues caused by inhibitors and cytotoxic compounds. Two model drugs, heptanol and doxorubicin, were introduced to 5 day cultures, and their effects on cardiac cell beating and viability were studied. Heptanol is a widely used reversible inhibitor of cell-to-cell coupling, which prevents gap-junctional permeability of Ca^{2+} and interrupts beating propagation.[37,38] Figure 5A shows the normalized synchronous beating amplitudes (in relation to untreated tissues of the same type) over 30 min from the start of the heptanol (4 mM) perfusion. A rapid disappearance of synchronous beating was observed on the pristine GelMA surface within 20 min, while beating persisted on CNT-GelMA. With increased CNT concentrations, more gradual disturbance to beating rhythm was observed. It took significantly longer for the tissues on CNT-GelMA to start sporadic beating (26−40 min *vs* 10 min) and stop beating (40−65 min *vs* 20 min) (Figure 5B). In other words, cardiomyocytes on CNT-GelMA continued to beat synchronously even after the gap-junctional beating propagation was inhibited, indicating that the conductive CNT network played a role in propagating calcium transient and action potential between cells, as illustrated schematically in Figure 5C.[7] The effect of heptanol was reversible since the beating characteristics returned to initial values after the removal of heptanol.

Upon perfusion of 300 μM doxorubicin into the growth chamber, tissues on pristine GelMA showed an immediate decrease (>50%) in the beating amplitude, as well as the beating rates (Figure 5D and Figure S8). Detached tissues and debris were observed after 6 h. In contrast, the amplitude and beat-to-beat variation of cardiac tissues on CNT-GelMA were not significantly effected by the same concentration of doxorubicin. MTS assay showed that the viable cell population (98.5%) on CNT-GelMA was significantly higher than that on pristine GelMA (79.6%) (Figure 5E), which suggests a protective role of CNT against oxidative stress. The generation of free oxygen radicals is believed to be the main mechanism for the cardiotoxicity of doxorubicin.[39] We suspect that CNTs acted as free radical scavengers through two mechanisms, adduct formation (covalent bonding with carbon or physisorption on CNT surface) and neutralization through electron transfer processes, as shown schematically in

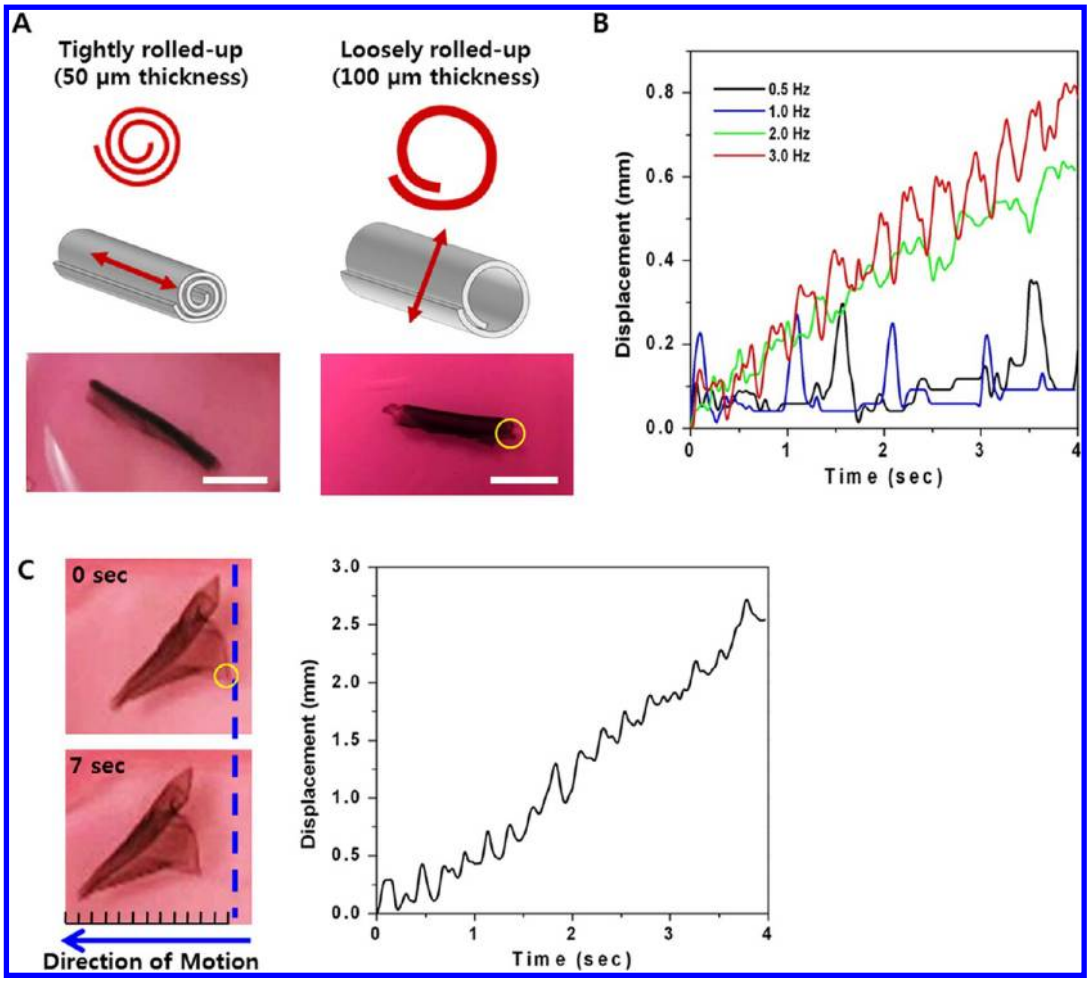

Figure 6. Engineered cardiac patches form free-standing 3D biohybrid actuators. (A) Schematic drawing of tubular actuators (tightly and loosely rolled-up forms) and their corresponding beating directions (red arrow), along with optical images of two samples. Scale bar is 5 mm. (B) Displacement of the tubular actuator (yellow circled tip in A) over time under electrical stimulation (square waveform, 1 V/cm, frequency = 0.5−3 Hz, 50 ms pulse width). (C) Spontaneous linear traveling of a triangular swimmer, as shown in optical images (at 0 and 7 s) and the displacement *vs* time plot. Ruler marking in B is 1 mm.

Figure 5F.[30,31] Adduct formation would reduce the spreading of radicals, and neutralization would reduce the activity of radicals and even facilitate breakdown of such species, which is similar to the catalytic decomposition of H_2O_2 to O_2 and H_2O shown in a previous report on nanoceria.[32]

Interestingly, after exposure to either heptanol or doxorubicin, the tissues on 5 mg/mL CNT-GelMA showed enhanced beating amplitudes and rates. Even though the exact mechanisms causing this phenomenon demand further investigation, we suspect that this phenomenon is correlated to the high electrical conductivity and the maximal protective effect of CNTs at a high concentration.

CNT-GelMA-Based 2D Cardiac Patches as Biohybrid Actuators. In addition to their therapeutic potential, *in vitro* cultured cardiac tissue constructs also showed promise in building biohybrid actuators and powering devices.[40,41] So far, such actuators have been largely limited to cell/tissue attached to highly stiff substrates, such as silicon and PDMS, for sufficient mechanical integrity. However, high substrate rigidity has been known to affect the contractile function of cardiac tissue/cells.[42] Since cardiac tissues cultured on CNT-GelMA were observed to have enhanced mechanical integrity, drastically lower excitation threshold, and more stable synchronous beating, we anticipate that such 2D cardiac patches can be released to form 3D biohybrid actuators with low stiffness and advantageous actuation behaviors, and therefore, the feasibility was investigated in this study.

After a square-shaped patch (1 cm^2) was detached from the glass substrate, it would spontaneously adopt one of two shapes in the cell medium, either tubular (rolled-up) or planar (folded). Two tubular actuators and a triangular swimmer are shown in Figure 6 as examples. All actuators displayed strong spontaneous and electrically stimulated motion. The exact mode of motion, however, differed depending on the patch thickness and the actuator's 3D form. Patches created on 50 μm thick CNT-GelMA rolled-up tightly and showed cyclic extension/contraction along the tube

axis (movies 1 and 2), while the thicker patches (100 μm) showed a loosely rolled-up form and mainly cyclic roll opening/closing (*i.e.*, pumping). The pumping frequency was precisely controllable by applying an external electric field (1 V/cm) at 0.5, 1, 2, and 3 Hz (movie 3). By tracking one tip of the tubular actuator (made on a 100 μm film) over time, as plotted in Figure 6B, we were able to study detailed frequency-dependent actuation behavior. At low frequencies (0.5 and 1 Hz), large amplitude and isolated pumping was observed following each applied pulse, and there was no overall translocation in space. At higher frequencies (2 and 3 Hz), small and continuous pumping was observed along with linear and rotational displacements of the sample. Higher beating frequency led to higher displacement velocity. The triangular swimmer, on the other hand, showed spontaneous cyclic planar extension/contraction at ~3 Hz and had a travel velocity about 17 mm/min (Figure 6C and movie 4). These results suggest that CNT-GelMA-based 2D cardiac patches have great potential as biohybrid actuators, similar to the previously reported muscular thin film actuators fabricated on much stiffer polydimethylsiloxane (PDMS) films coated with fibronectin.[41,43] In comparison, cardiac patches cultured on pristine GelMA ruptured after 5 days and could not generate an intact patch (movie 5). Given its ability to scavenge harmful toxins, its enhanced mechanical and electrical properties, and its ability to yield functional cardiac patches, we envision a wide range of applications for the engineered CNT-GelMA films.

CONCLUSIONS

In summary, we demonstrated that the addition of multiwalled CNTs into photo-cross-linkable GelMA led to a hybrid hydrogel (CNT-GelMA) with significantly altered electrophysiological and mechanical properties. Compression modulus and electrical conductivity of the gels, as well as key indicators of their biocompatibility (*e.g.*, percentage cell retention and viability, cell alignment index), showed clear dependence on CNT concentration. We systematically evaluated CNT-GelMA hybrid gels with 1, 3, and 5 mg/mL CNTs and used pristine 5% GelMA as a reference in this study. CNTs formed electrically conductive and collagen fibril-like nanofibers bridging pores, which mechanically strengthened the gel, promoted cardiac cell adhesion and maturation, and improved cell–cell electrical coupling. Cross-striation of F-actin and partial cell alignment were evident on CNT-GelMA but not on pristine GelMA hydrogels. Ultrathin 2D cardiac patches fabricated by seeding neonatal rat cardiomyocytes onto CNT-GelMA thin films showed strong spontaneous and stimulated synchronous beating. In addition, we observed protective effect of the CNT-GelMA scaffold against doxorubicin (cardio-toxic) and heptanol (cardio-inhibitor). To our knowledge, this is the first report on a protective cardiac scaffold. When released from glass substrates, the 2D cardiac patches (centimeter size) formed 3D soft actuators with controllable linear contractile, pumping, and swimming actuation behaviors. CNT concentration of 3 mg/mL led to tissues with optimal electrophysiological functions, while 5 mg/mL showed the maximal protective effect. Compared to existing scaffold materials, CNT-GelMA stands out for its multifunctionality. Furthermore, the evidently strong cell–CNT interactions will allow the conductive CNT networks to be embedded into engineered tissues after the degradation of the gelatin matrix.[7,27,29]

EXPERIMENTAL METHODS

Materials. A carboxyl acid group functionalized multiwalled CNT (30 ± 15 nm in diameter and 5–20 μm in length, 95% purity) was purchased from NanoLab Inc. Methacrylic anhydride, gelatin (type A), 3-(trimethoxysilyl)propyl methacrylate (TMSPMA), 1-heptanol, and doxorubicin were purchased from Sigma-Aldrich. The photoinitoator, 2-hydroxy-1-(4-(hydroxyethoxy)-phenyl)-2-methyl-1-propanone (Irgacure 2959) was purchased from CIBA Chemical.

Methacrylated Gelatin (GelMA) Synthesis. GelMA was synthesized following a previously reported method with minor modifications.[18] Gelatin (10% w/v) was dissolved into Dulbecco's phosphate buffered saline (DPBS) at 50 °C. To modify the lysine group on gelatin chains, methacrylate anhydride (0.8 mL per gram of gelatin) was added to the gelatin solution at 50 °C. After 2 h, the solution was diluted with DPBS to stop the reaction. To remove unreacted methacrylate anhydride and salt, the diluted solution was dialyzed in a distilled water bath for 5 days at 40 °C (molecular weight cutoff = 12–14 kDa). This GelMA solution was filtered (0.2 μm) and then frozen using liquid nitrogen. The frozen GelMA was lyophilized for 5 days to obtain the white foam GelMA for future use. The degree of methacrylation, which is about 90% in this work, was quantified by following a previously reported method using ^{1}H NMR.[18]

Preparation of CNT-GelMA Thin Film. To prepare prepolymer solution, GelMA was dissolved in DPBS (2% w/v) at 50 °C for 10 min. Carboxyl acid group functionalized multiwalled CNTs (5 mg/mL) were added to the above GelMA solution. To obtain a black ink-like solution containing GelMA-coated CNTs, this solution was then sonicated (VCX 400, 80 W, 2 s on and 1 s off) for 1 h in a water bath. A selected amount of this solution was then added to a GelMA solution (5% w/v) containing 0.5% photoinitiator to make a prepolymer solution for gelation, with a final target concentration of CNTs at 0, 1, 3, and 5 mg/mL. To prepare a hydrogel thin film, 10 μL prepolymer solution was placed between two 50 μm tall spacers, covered with a TMSPMA-coated glass slide. The prepolymer solution was exposed to UV light (6.9 mW/cm^2, 360–480 nm). The transmittance of the CNT-GelMA prepolymer solution was measured with a UV spectrophotometer (Shimadzu, UV-2450, Japan) (Figure S1). The UV exposure times were optimized to be 5, 50, 80, and 120 s for making hydrogels with 0, 1, 3, and 5 mg/mL of CNTs, respectively.

Characterization of Hydrogel Thin Film. To measure the mechanical properties of the hydrogel thin film, 150 μm thick swollen samples in DPBS were tested on a Nano-UTM (Nanobionix) machine. All tests were carried out using a spherical indenter with a radius of 1 mm to generate a maximum load of 0.3 mN at

an approaching rate of 0.1 um/s. The sample size was 5 gels per group. For impedance measurements, the hydrogel films were pressed between two gold-coated glass slides with an AC bias sweeping between 40 Hz and 1 MHz. The impedance at each frequency was recorded. The surfaces of the hydrogel films were examined using SEM (Hitachi model S4700, Japan). The SEM samples were prepared by freezing swollen hydrogel films in liquid nitrogen followed by lyophilization. The lyophilized samples were then coated with Pt/Pd. For SEM imaging of seeded cells on the hydrogel films, cardiomyocytes were grown for 5 days. Before freezing the sample in liquid nitrogen, the sample was treated in glutaraldehyde solution (2.5%) for 2 h.

Cell Isolation and Culture. Neonatal rat ventricular cardiomyocytes were isolated from 2 day old Sprague−Dawley rats following a well-established protocol approved by the Institute's Committee on Animal Care.[44] Cardiomyocytes were used immediately after their isolation and enrichment through 2 h preplating. The cardiac cells were seeded onto either GelMA or CNT-GelMA (10 mm × 10 mm, 7.5×10^5 cells/well). The cell-seeded samples were cultured in Dulbecco's modified Eagle medium (DMEM, Gibco, USA) containing 10% fetal bovine serum (FBS, Gibco, USA), 1% L-glutamine (Gibco, USA), and 100 units/mL penicillin-streptomycin (Gibco, USA) up to 9 days without electric field stimulation.

Cell Characterization. A live/dead assay (Invitrogen, USA) was used according to the manufacturer's instructions. To determine the viability, the fluorescence image was taken using a fluorescence microscope (Nikon, Eclipse TE 2000U, Japan). The number of live/dead cells was measured by ImageJ software from 10 randomly selected areas of 3 gels for each group. MTS assays (CellTiter 96 Aqueous One Solution, Promega, USA) and DNA quantification (Quant-iT PicoGreen, Invitrogen, USA) were performed according to the manufacturer's instructions with three samples of each group to determine the proliferation of cells on hydrogels. To do immunocytochemistry, cultured cells were fixed in 4% paraformaldehyde for 30 min at room temperature. After fixation, cells were treated with 0.15% Triton X-100 for 30 min. The samples were treated with Alexa Fluor 488 phalloidin (1:40 dilution) and DAPI (1:10000 dilution) in DPBS for 40 min. Cardiac tissues were stained with three different kinds of primary antibodies (for sarcomeric α-actinin, Troponin I, connexin 43) at 1:200 dilution in blocking buffer for 24 h at 4 °C. This sample was treated with secondary antibody (1:200 dilution) in goat serum for 40 min. After washing with DPBS, this sample was counterstained with DAPI (1:10000) dilution in DPBS for 40 min at room temperature. These stained samples were then imaged with an inverted laser scanning confocal microscope (Leica SP5X MP, Germany).

Western Blotting. The expression levels of the special proteins related to the contractile function of cardiac tissue, such as Cx 43, Troponin I, and sarcomeric α-actinin, were quantified using Western blot assays. The extracted proteins were size-fractioned by sodium dodecylsulfate polyacrylamide gel electrophoresis (SDS-PAGE). This gel was transferred to nitrocellulose membranes, and then, the membranes were treated with antibodies against corresponding proteins and normalized against GAPDH. At least three cardiac patches were tested from each group. Densitometric analysis was carried out using ImageJ analysis software (NIH).

Electrophysiology Assessment. The microscope was equipped with a temperature control chamber at 37 °C. The image of the cultured cardiomyocytes was acquired with a CCD camera attached to the microscope. The beating video was obtained using a video capture program. The video sequences were digitized at a rate of 20 frames per second. We have previously developed an image processing program using MATLAB (MathWorks Inc., Natick, MA).[45] First, the reference image, which was taken from the first frame, and the images from consecutive frames were transformed to binary images and stored as two different matrices. To obtain an image difference matrix, we subtracted each consecutive frame image matrix from the reference image matrix after transformation. The image difference value was summed from the absolute values of each element in the image difference matrix. Larger difference value of the image reflects greater change between the reference and the consecutive frame images. The sample size was 6 gels per group for spontaneous beating analysis.

We used a modified carbon electrode system based on established protocols[46] to assess the response of cardiomyocytes to electric field stimulation. The electric pulse generator applied biphasic square waveforms with 50 ms pulses of 0−7 V/cm at 0.5, 1, 2, and 3 Hz to a sample positioned between two carbon electrodes within the test chamber. We decided the excitation threshold which is the minimum voltage observed to initiate synchronous contractions at each frequency. The video was recorded using 20 frames per second video camera (Sony XCD-X710) and a microscope (Nikon, Eclipse TE 2000U, Japan) at 10× magnification.

To assess the effects of drugs, 4 mM 1-heptanol and 300 μM doxorubicin were dissolved in culture medium and added to the cultured cardiomyocyte samples. The changes in beating amplitude, beating rate, and beat-to-beat variation were measured by video image-based analysis every 2 min. Control experiments were performed before the introduction of drugs. We normalized the parameters obtained from the samples treated with the drugs to the values obtained from the control samples. The result was obtained from 3 gels per group.

Study of Biohybrid Actuators. The 2D cardiac patches would be naturally released after 7−8 days of culturing. To measure actuation behavior, the biohybrid actuators were conducted at room temperature (~20 °C) in culture medium. Movies of biohybrid actuators were taken with a Panasonic HDC-HS9 digital camera capable of video recording (1920 × 1080 pixels, 24 fps). To control actuation, the electric pulse generator applied biphasic square wave forms with 50 ms pulses of 1 V/cm at 0.5, 1, 2, and 3 Hz to a sample placed between two platinum wire electrodes (spacing ~3 cm) in culture medium. Analysis of actuation was performed in a postprocessing step by tracking the frame-to-frame displacement with an image processing software. The conversion factor from pixels to micrometers was calculated for each video clip using the millimeter ruler included in the field of view for calibration.

Statistical Analysis. To analyze statistical significance, we used a one-way ANOVA where appropriate (GraphPad Prism 5.02, GraphPad Software). Error bar represents the mean ± standard deviation (SD) of measurements performed on each sample group. To determine whether a significant difference exists between specific treatments, we used Tukey's multiple comparison tests ($p < 0.05$).

Conflict of Interest: The authors declare no competing financial interest.

Acknowledgment. This paper was supported by the Institute for Soldier Nanotechnology, National Institutes of Health (HL092836, EB02597, AR057837, HL099073), the National Science Foundation (DMR0847287), the Office of Naval Research Young Investigator award, ONR PECASE Award, and the National Research Foundation of Korea Grant funded by the Korean Government (NRF-2010-220-D00014).

Supporting Information Available: Fabrication of hydrogel thin film, SEM images, live/dead images, analysis of cell alignment, confocal images, drug test. This material is available free of charge *via* the Internet at http://pubs.acs.org.

REFERENCES AND NOTES

1. Chien, K. R.; Domian, I. J.; Parker, K. K. Cardiogenesis and the Complex Biology of Regenerative Cardiovascular Medicine. *Science* **2008**, *322*, 1494–1497.
2. Dvir, T.; Timko, B. P.; Kohane, D. S.; Langer, R. Nanotechnological Strategies for Engineering Complex Tissues. *Nat. Nanotechnol.* **2011**, *6*, 13–22.
3. Nowak, A. P.; Breedveld, V.; Pakstis, L.; Ozbas, B.; Pine, D. J.; Pochan, D.; Deming, T. J. Rapidly Recovering Hydrogel Scaffolds from Self-Assembling Diblock Copolypeptide Amphiphiles. *Nature* **2002**, *417*, 424–428.
4. Engelmayr, G. C., Jr.; Cheng, M.; Bettinger, C. J.; Borenstein, J. T.; Langer, R.; Freed, L. E. Accordion-like Honeycombs for Tissue Engineering of Cardiac Anisotropy. *Nat. Mater.* **2008**, *7*, 1003–1010.

5. You, J. O.; Rafat, M.; Ye, G. J.; Auguste, D. T. Nanoengineering the Heart: Conductive Scaffolds Enhance Connexin 43 Expression. *Nano Lett.* **2011**, *11*, 3643–3648.
6. Liau, B.; Zhang, D.; Bursac, N. Functional Cardiac Tissue Engineering. *Regen. Med.* **2012**, *7*, 187–206.
7. Dvir, T.; Timko, B. P.; Brigham, M. D.; Naik, S. R.; Karajanagi, S. S.; Levy, O.; Jin, H.; Parker, K. K.; Langer, R.; Kohane, D. S. Nanowired Three-Dimensional Cardiac Patches. *Nat. Nanotechnol.* **2011**, *6*, 720–725.
8. Silva, G. A.; Czeisler, C.; Niece, K. L.; Beniash, E.; Harrington, D. A.; Kessler, J. A.; Stupp, S. I. Selective Differentiation of Neural Progenitor Cells by High-Epitope Density Nanofibers. *Science* **2004**, *303*, 1352–1355.
9. Lutolf, M. P.; Hubbell, J. A. Synthetic Biomaterials as Instructive Extracellular Microenvironments for Morphogenesis in Tissue Engineering. *Nat. Biotechnol.* **2005**, *23*, 47–55.
10. Shim, J.; Grosberg, A.; Nawroth, J. C.; Parker, K. K.; Bertoldi, K. Modeling of Cardiac Muscle Thin Films: Pre-stretch, Passive and Active Behavior. *J. Biomech.* **2012**, *45*, 832–841.
11. Lee, C. K.; Shin, S. R.; Mun, J. Y.; Han, S. S.; So, I.; Jeon, J. H.; Kang, T. M.; Kim, S. I.; Whitten, P. G.; Wallace, G. G.; *et al.* Tough Supersoft Sponge Fibers with Tunable Stiffness from a DNA Self-Assembly Technique. *Angew. Chem., Int. Ed.* **2009**, *48*, 5116–5120.
12. Pieperhoff, S. Gene Mutations Resulting in the Development of ARVC/D Could Affect Cells of the Cardiac Conduction System. *Front. Physiol.* **2012**, *3*, 1–4.
13. Garzon, A.; Grigoriev, R. O.; Fenton, F. H. Model-Based Control of Cardiac Alternans in Purkinje Fibers. *Phys. Rev. E* **2011**, *84*, 041927.
14. Mooney, E.; Mackle, J. N.; Blond, D. J.; O'Cearbhaill, E.; Shaw, G.; Blau, W. J.; Barry, F. P.; Barron, V.; Murphy, J. M. The Electrical Stimulation of Carbon Nanotubes To Provide a Cardiomimetic Cue to MSCs. *Biomaterials* **2012**, *33*, 6132–6139.
15. Drury, J. L.; Mooney, D. J. Hydrogels for Tissue Engineering: Scaffold Design Variables and Applications. *Biomaterials* **2003**, *24*, 4337–4351.
16. Sekine, H.; Shimizu, T.; Okano, T. Myocardial Tissue Engineering: Toward a Bioartificial Pump. *Cell Tissue Res.* **2012**, *347*, 775–782.
17. Zorlutuna, P.; Annabi, N.; Camci-Unal, G.; Nikkhah, M.; Cha, J. M.; Nichol, J. W.; Manbachi, A.; Bae, H.; Chen, S.; Khademhosseini, A. Microfabricated Biomaterials for Engineering 3D Tissues. *Adv. Mater.* **2012**, *24*, 1782–1804.
18. Nichol, J. W.; Koshy, S. T.; Bae, H.; Hwang, C. M.; Yamanlar, S.; Khademhosseini, A. Cell-Laden Microengineered Gelatin Methacrylate Hydrogels. *Biomaterials* **2010**, *31*, 5536–5544.
19. Aubin, H.; Nichol, J. W.; Hutson, C. B.; Bae, H.; Sieminski, A. L.; Cropek, D. M.; Akhyari, P.; Khademhosseini, A. Directed 3D Cell Alignment and Elongation in Microengineered Hydrogels. *Biomaterials* **2010**, *31*, 6941–6950.
20. Gauvin, R.; Chen, Y. C.; Lee, J. W.; Soman, P.; Zorlutuna, P.; Nichol, J. W.; Bae, H.; Chen, S.; Khademhosseini, A. Microfabrication of Complex Porous Tissue Engineering Scaffolds Using 3D Projection Stereolithography. *Biomaterials* **2012**, *33*, 3824–3834.
21. Shin, S. R.; Bae, H.; Cha, J. M.; Mun, J. Y.; Chen, Y.-C.; Tekin, H.; Shin, H.; Farshchi, S.; dokmeci, M. R.; Shirley, T.; *et al.* Carbon Nanotube Reinforced Hybrid Microgels as Scaffold Materials for Cell Encapsulation. *ACS Nano* **2012**, *6*, 362–372.
22. Hussain, M. A.; Kabir, M. A.; Sood, A. K. On the Cytotoxicity of CNT. *Curr. Sci.* **2009**, *96*, 664–673.
23. Al-Jamal, K. T.; Nunes, A.; Methven, L.; Ali-Boucetta, H.; Li, S.; Toma, F. M.; Herrero, M. A.; Al-Jamal, W. T.; Ten Eikelder, H. M.; Foster, J.; *et al.* Degree of Chemical Functionalization of Carbon Nanotubes Determines Tissue Distribution and Excretion Profile. *Angew. Chem., Int. Ed.* **2012**, *51*, 6389–6393.
24. Tang, A. C.; Chang, M. Y.; Tang, Z. C.; Li, H. J.; Hwang, G. L.; Hsieh, P. C. The Treatment of Acute Thromboembolism in Mice Using Heparin-Conjugated Carbon Nanocapsules. *ACS Nano* **2012**, *6*, 6099–6107.
25. Robinson, J. T.; Hong, G.; Liang, Y.; Zhang, B.; Yaghi, O. K.; Dai, H. *In Vivo* Fluorescence Imaging in the Second Near-Infrared Window with Long Circulating Carbon Nanotubes Capable of Ultrahigh Tumor Uptake. *J. Am. Chem. Soc.* **2012**, *134*, 10664–10669.
26. W.S., K. N.; O'Connell, M.; Wisdom, J. A.; Dai, H. Carbon Nanotubes as Multifunctional Biological Transporters and Near-Infrared Agents for Selective Cancer Cell Destruction. *Proc. Natl. Acad. Sci. U.S.A.* **2005**, *102*, 11600–11605.
27. Martinelli, V.; Cellot, G.; Toma, F. M.; Long, C. S.; Caldwell, J. H.; Zentilin, L.; Giacca, M.; Turco, A.; Prato, M.; Ballerini, L.; *et al.* Carbon Nanotubes Promote Growth and Spontaneous Electrical Activity in Cultured Cardiac Myocytes. *Nano Lett.* **2012**, *12*, 1831–1838.
28. Lovat, V.; Pantarotto, D.; Lagostena, L.; Cacciari, B.; Grandolfo, M.; Righi, M.; Spalluto, G.; Prato, M.; Ballerini, L. Carbon Nanotube Substrates Boost Neuronal Electrical Signaling. *Nano Lett.* **2005**, *5*, 1107–1110.
29. Cellot, G.; Cilia, E.; Cipollone, S.; Rancic, V.; Sucapane, A.; Giordani, S.; Gambazzi, L.; Markram, H.; Grandolfo, M.; Scaini, D.; Gelain, F.; *et al.* Carbon Nanotubes Might Improve Neuronal Performance by Favouring Electrical Shortcuts. *Nat. Nanotechnol.* **2008**, *4*, 126–133.
30. Injac, R.; Perse, M.; Cerne, M.; Potocnik, N.; Radic, N.; Govedarica, B.; Djordjevic, A.; Cerar, A.; Strukelj, B. Protective Effects of Fullerenol $C_{60}(OH)_{24}$ Against Doxorubicin-Induced Cardiotoxicity and Hepatotoxicity in Rats with Colorectal Cancer. *Biomaterials* **2009**, *30*, 1184–1196.
31. Galano, A. Carbon Nanotubes as Free-Radical Scavengers. *J. Phys. Chem. C* **2008**, *112*, 8922–8927.
32. Pagliari, F.; Mandoli, C.; Forte, G.; Magnani, E.; Pagliari, S.; Nardone, G.; Licoccia, S.; Minieri, M.; Di Nardo, P.; Traversa, E. Cerium Oxide Nanoparticles Protect Cardiac Progenitor Cells from Oxidative Stress. *ACS Nano* **2012**, *6*, 3767–3775.
33. Wang, H.-B.; Dembo, M.; WAng, Y.-L. Substrate Flexibility Regulates Growth and Apoptosis of Normal but Not Transformed Cells. *Am. J. Physiol.* **2000**, *279*, C1345–C1350.
34. Huang, N. F.; Patel, S.; Thakar, R. G.; Wu, J.; Hsiao, B. S.; Chu, B.; Lee, R. J.; Li, S. Myotube Assembly on Nanofibrous and Micropatterned Polymers. *Nano Lett.* **2006**, *6*, 537–542.
35. Hazeltine, L. B.; Simmons, C. S.; Salick, M. R.; Lian, X.; Badur, M. G.; Han, W.; Delgado, S. M.; Wakatsuki, T.; Crone, W. C.; Pruitt, B. L.; *et al.* Effects of Substrate Mechanics on Contractility of Cardiomyocytes Generated from Human Pluripotent Stem Cells. *Int. J. Cell. Biol.* **2012**, 508294–508306.
36. Bhana, B.; Iyer, R. K.; Chen, W. L.; Zhao, R.; Sider, K. L.; Likhitpanichkul, M.; Simmons, C. A.; Radisic, M. Influence of Substrate Stiffness on the Phenotype of Heart Cells. *Biotechnol. Bioeng.* **2010**, *105*, 1148–1160.
37. Takens-Kwak, B. R.; Jongsma, H. J.; Rook, M. B.; Van Ginneken, A. C. Mechanism of Heptanol-Induced Uncoupling of Cardiac Gap Junctions: A Perforated Patch-Clamp Study. *Am. J. Physiol.* **1992**, *262*, C1531–C1538.
38. Rodriguez-Sinovas, A.; Garcia-Dorado, D.; Ruiz-Meana, M.; Soler-Soler, J. Protective Effect of Gap Junction Uncouplers Given during Hypoxia against Reoxygenation Injury in Isolated Rat Hearts. *Am. J. Physiol.* **2006**, *290*, H648–H656.
39. Mukhopadhyay, P.; Rajesh, M.; Batkai, S.; Kashiwaya, Y.; Hasko, G.; Liaudet, L.; Szabo, C.; Pacher, P. Role of Superoxide, Nitric Oxide, and Peroxynitrite in Doxorubicin-Induced Cell Death *in Vivo* and *in Vitro*. *Am. J. Physiol.* **2009**, *296*, H1466–H1483.
40. Ricotti, L.; Menciassi, A. Bio-Hybrid Muscle Cell-Based Actuators. *Biomed. Microdevices* **2012**, *14*, 987–998.
41. Feinberg, A. W.; Feigel, A.; Shevkoplyas, S. S.; Sheehy, S.; Whitesides, G. M.; Parker, K. K. Muscular Thin Films for Building Actuators and Powering Devices. *Science* **2007**, *317*, 1366–1370.
42. Chan, V.; Jeong, J. H.; Bajaj, P.; Collens, M.; Saif, T.; Kong, H.; Bashir, R. Multi-Material Bio-Fabrication of Hydrogel Cantilevers and Actuators with Stereolithography. *Lab Chip* **2012**, *12*, 88–98.
43. Nawroth, J. C.; Lee, H.; Feinberg, A. W.; Ripplinger, C. M.; McCain, M. L.; Grosberg, A.; Dabiri, J. O.; Parker, K. K.

A Tissue-Engineered Jellyfish with Biomimetic Propulsion. *Nat. Biotechnol.* **2012**, *30*, 792–797.
44. Khademhosseini, A.; Eng, G.; Yeh, J.; Kucharczyk, P. A.; Langer, R.; Vunjak-Novakovic, G.; Radisic, M. Microfluidic Patterning for Fabrication of Contractile Cardiac Organoids. *Biomed. Microdevices* **2007**, *9*, 149–157.
45. Kim, S. B.; Bae, H.; Cha, J. M.; Moon, S. J.; Dokmeci, M. R.; Cropek, D. M.; Khademhosseini, A. A Cell-Based Biosensor for Real-Time Detection of Cardiotoxicity Using Lensfree Imaging. *Lab Chip* **2011**, *11*, 1801–1807.
46. Tandon, N.; Cannizzaro, C.; Chao, P. H.; Maidhof, R.; Marsano, A.; Au, H. T.; Radisic, M.; Vunjak-Novakovic, G. Electrical Stimulation Systems for Cardiac Tissue Engineering. *Nat. Protoc.* **2009**, *4*, 155–173.